Published in final edited form as:
Dalton Trans. 2016 April 21; 45(15): 6732–6738. doi:10.1039/c5dt04502a.

Photochemical hydrogen production and cobaloximes: influence of cobalt axial *N*-ligand on the system stability

Athanassios Panagiotopoulos[1], **Kalliopi Ladomenou**[1], **Dongyue Sun**[2], **Vincent Artero**[2,*], and **Athanassios G. Coutsolelos**[1,*]

[1]Laboratory of Bioinorganic Chemistry, Department of Chemistry, University of Crete, Voutes Campus, 70013 Heraklion, Crete, Greece

[2]Laboratoire de Chimie et Biologie des Métaux, Université Grenoble Alpes, CNRS, CEA, 17 rue des Martyrs, 38000 Grenoble, France

Abstract

We report on the first systematic study of cobaloxime-based hydrogen photoproduction in mixed pH 7 aqueous/acetonitrile solutions and demonstrate that H_2 evolution can be tuned through electronic modifications of the axial cobalt ligand or through introduction of TiO_2 nanoparticles. The photocatalytic systems consist of various cobaloxime catalysts [$Co(dmgH)_2(L)Cl$] (L = nitrogen-based axial ligands) and a water soluble porphyrin photosensitizer. They were assayed in the presence of triethanolamine as sacrificial electron donor. Optimal turnover numbers related to photosensitizer are obtained with electron-rich axial ligands such as imidazole derivatives (1131 TONs with N-methyl imidazole). Lower stabilities are observed with various pyridine axial ligands (443 TONs for para-methylpyridine), especially for those containing electron-acceptor substituents. Interestingly, when L is the para-carboxylatopyridine the activity of the system is increased from 40 to 223 TONs in the presence of TiO_2 nanoparticles

Keywords

Porphyrins; Metallo-porphyrins; Hydrogen production; Photocatalysis; Cobaloxime

Introduction

The development and optimization of methods allowing storing renewable energy sources such as sunlight is a major challenge to tackle both problems of decreasing stocks of fossil fuels and accumulating CO_2 greenhouse gas in the atmosphere.1 A fairly promising path for the efficient conversion of solar energy into fuels, so-called solar fuels,2 is to develop efficient photocatalytic systems for hydrogen (H_2) production from water,3, which constitutes a great endeavor of artificial photosynthesis. Typical photocatalytic systems contain distinct photosensitizer and catalyst, the former achieving light harvesting and initial charge separation. The system is generally assessed in the presence of a sacrificial electron donor, which allows decoupling the optimization of reductive and oxidative sides of water

Athanassios G. Coutsolelos, www.chemistry.uoc.gr/coutsolelos, acoutsol@uoc.gr. **Vincent Artero**, http://www.solhycat.com, vincent.artero@cea.fr.

Europe PMC Funders Author Manuscripts

splitting. Great challenges in the field of photocatalytic hydrogen production include the development of systems based on earth-abundant materials together with the enhancement of their activity and durability.4, 5 Bioinspiration is a key feature in the design of such molecular systems. Water soluble porphyrins and metallated porphyrins, due to their similarity to natural photosynthetic dyes, are excellent candidates for efficient absorption of photons and charge separation in this context.6, 7 In addition cobaloximes gained great attention in the past ten years and have been used as catalysts in photocatalytic systems because of their low-cost, high activity and straightforward synthesis.8–30

Recently our group reported an homogeneous system involving a porphyrin sensitizer and a cobaloxime catalyst [Co(dmgH)$_2$pyCl] (dmgH$_2$ = dimethylglyoxime) for photoinduced hydrogen evolution from water.31 Upon continuous visible irradiation of mixed 50/50 acetonitrile/H_2O solutions hydrogen was produced with the best result obtained at pH 7 with a TON of 320 with respect to the porphyrin after 35 h.9, 10, 12, 32 In this study, we use same conditions to examine the influence of different axial ligands on the cobaloxime catalyst.

Results and Discussion

A series of cobalt bisdimethylglyoximato complexes [Co^{III}(dmgH)$_2$(L)Cl] (**1**-**10**) with different pyridine and imidazole axial ligands (Figure 1) were synthesized according to the literature procedure by dissolving $CoCl_2 \cdot 6H_2O$, 2 equivalents of dimethylglyoxime and 1 equivalent of NaOH in 95% ethanol at 70°C.33 Then, 1 equivalent of the appropriate ligand was added. All complexes were isolated in excellent yields after work-up (see Experimental Section for details). Compound [Co(dmgH)(dmgH$_2$)Cl$_2$] (**10**) was prepared and used as reference.34 Cyclic voltammograms (CVs) were recorded in DMF and displayed an irreversible reduction process assigned to the Co(III)/Co(II) transition and a reversible wave assigned to the Co(II)/Co(I) process. All cobalt complexes show similar behaviors (Table 1). Figure 2 (top) shows cyclic voltammograms of selected compounds in the series. We first note that the potential of the reversible Co(II)/Co(I) process depends on the nature of the axial *N* ligand. Secondly, on the return scan a novel Co(II) to Co(III) process is observed, the position of which also depends on the nature of the axial ligand. In both cases, a more electron-donating (respectively electron-withdrawing) substituent of the pyridine axial ligand results in a cathodic (respectively anodic) shift of the potential of the redox process. Collectively, these data indicate that the chloride ligand is reductively eliminated at the Co(II) state and that the *N*-ligand remains coordinated in the Co(II) state and probably also in the Co(I) state since the wave is electrochemically reversible. Multiple scan measurements indicate that the chloride ligand only slowly rebinds to the Co(III) center (Figure 2, bottom).

Compounds **1-10** were characterized using FTIR spectroscopy. Table 1 gathers the wavenumbers corresponding to the Co-N_{axial} and Co-Cl stretching vibrations.35 It appears clearly that the Co-Cl bond strength decreases when the Co-N_{axial} bond strength increases, following an increase of the basicity of the axial *N*-ligand.

Photocatalytic hydrogen production using **1-10** as catalysts, zinc *meso*-tetrakis (1-methylpyridinium-4-yl) porphyrin chloride [$ZnTMPyP^{4+}$]Cl_4 as photosensitizer (**PS**) and triethanolamine (TEOA) as sacrificial donor was measured as a function of time. All experiments were carried out under similar conditions as in our previously published work but with a slightly different setup (detailed conditions are provided in Experimental Section).31 The pH was adjusted to 7 through addition of aqueous HCl. We note that, under such conditions, **10** is likely deprotonated with consequent detachment of (at least) one axial chloride ligand and ligation of neutral solvent molecule(s). Therefore this compound displays a H^+-annulated structure similar to other cobaloximes. The activity for each photocatalytic system is measured in turnover number versus photosensitizer (TON), which evolves as a function of time. The results are gathered in Figures 3 and 4. Two photocatalytic behaviors can be distinguished. First cobaloximes containing imidazole or pyridine ligand with donor substituents prove highly active and stable. By contrast, cobaloximes without pyridine ligands (for example with two chloride ligands) or with electron-withdrawing group-substituted pyridine ligands display significantly lower stability. Another difference is seen in the time-profile of H_2 evolution: while the less stable systems immediately produce H_2 on irradiation, the more stable systems display an S-shaped activity curve with lower initial rates of H_2 photoproduction.

N-methyl imidazole-containing catalyst **9** proved to be the most stable one of the cobaloximes with 1135 turnovers achieved for H_2 production after 50 hours of irradiation. Moreover, catalyst **8**, containing imidazole axial ligand, exhibits a total TON of 565 under similar conditions. Using pyridine ligands with electron donating groups as axial ligands also yield highly effective catalysts **4-7** exceeding the activity of **3** (TON = 320, Figure 3). Such an activity can be rationalized on the basis of the basicity of these N-based aromatic ligands, resulting in various electron-donor ability, after binding to cobalt. The higher pK_a of imidazole derivatives (Table 2) correlates well with the higher stability of the corresponding systems compared to pyridine-based ones. In addition, the performances of systems using **3-5** follow their pK_a values: the activity is increased following the order **5** (pK_a = 6.02) > **4** (pK_a=5.30) > **3** (pK_a =5.22).

Pyridine ligands with electron withdrawing groups and therefore lower pK_a values form less effective catalysts **1-2** (Figure 3) as compared to **3**. Because of its higher pK_a value **2** is expected to produce more H_2 than **1**. This is however not the case, maybe due to the formation of carboxylate species under the conditions used. Addition of TiO_2 nanoparticles into the solution allows the attachment of the catalysts at the surface of the particles26 and the catalytic performance of **2** is improved by a five-fold factor. Upon irradiation of the system up to 223 turnovers of H_2 obtained after 29 hours of irradiation. We posit that binding of the carboxylate group of the pyridine ligand to TiO_2 forms a mixed organic-inorganic ester26 with lower electron-withdrawing property but we cannot exclude the fact that TiO_2 particles partake in catalysis as electron reservoirs as previously demonstrated by Reisner, Durrant and coworkers.28, 36 We note that cobaloxime **6** proves inactive under such conditions. This can be attributed to the amine being protonated at pH=7 (pK_a = 9.12) therefore resulting in a strong electron-withdrawing ammonium group.37 The absence of catalytic activity observed with 4-hydroxypyridine derivative (**7**), may be due to the

formation of a 4-pyridone tautomer.38 The above results are in agreement with literature data reported by us18 and by Reisner and coworkers.39 Both studies indeed demonstrated enhanced electrochemical H_2 evolution activity for cobaloximes with electron-enriched axial ligands.

Systems containing catalysts **1**, **10** and **2-TiO$_2$** rapidly produce H_2 immediately upon irradiation, but H_2 evolution stops after 10 h. By contrast, the other series of catalysts, achieving higher turnover number, display a significantly lower initial rate for H_2 production than the second series. The highest TON is also achieved after a longer irradiation time (~50 hours).

The efficiency and stability of a homogeneous photochemical system for H_2 evolution is actually controlled by four main processes: (i) light harvesting, charge separation and generation of a reducing agent; (ii) catalyst reductive activation; (iii) H_2 evolution catalysis and (iv) deactivation processes. Under the conditions used, the efficiency of (i), as well as the rate of a possible deactivation of the photosensitizer are likely constant. This is quite different for process (ii). In our previous work involving the same porphyrin photosensitizer, 31 we used transient absorption measurements to show that that the triplet excited state of the porphyrin **PS*** contributes to H_2 production. However, the potential of this state can be estimated to –0.45 V vs NHE40 so that only electron transfer to Co(III) generating the Co(II) species is thermodynamically possible. The formation of the Co(I) state of the catalyst can therefore only be possible from the reduced porphyrin photosensitizer **PS$^-$** ($E° \sim$ –0.85 V vs NHE 40), generated through reductive quenching by TEOA. The catalytic mechanism for H_2 production mediated by cobaloximes indeed involves formation of Co(III)-hydride intermediates by protonation of Co(I). Next, Co(III)-hydrides are reduced into Co(II)-hydrides through electron transfer either from the photosensitizer or from Co(I) species.10, 41–43 H_2 is then formed through protonation of these Co(II)-H species regenerating the cobaloxime in the Co(II) state.

Comparing redox potentials measured in distinct solvents is always challenging. In the present case, we use a mixture of water and acetonitrile in the presence of a high concentration of TEOA so that extrapolations are almost impossible. It seems however from the comparison of E^0(**PS$^-$/PS**) and $E^0(Co^{II}/Co^{I})$ that the driving force for the formation of Co(I) from **PS$^-$** is quite small. Under such conditions, small variations of the redox potential of the Co(II)/Co(I) process due to the influence of the axial ligand can control the reduction activation process (ii) and explain the large difference in reactivity observed within the series. In particular, the lower initial rates for H_2 evolution observed with the catalysts containing the stronger axial ligands correspond to a lower driving force for electron transfer from the reduced photosensitizer to the Co(II) catalyst.

In addition, the nature of the axial ligand alters the properties of the intermediate Co(III)-hydride derivative, both through a modification of the Co(III)-H/Co(II)-H redox potential and through a modification of the nucleophilicity of the Co(II)-H derivative.18, 44–46 In particular, as said above, electron-donating axial ligands enhance the rate of H_2 evolution catalysis (process iii).18, 39 This effect is however not observed here since (ii) is the rate determining process. We note that this behavior contrasts with that described for a related

photocatalytic diimine-dioxime cobalt system, in which the introduction of an electron-withdrawing axial ligand capable of stabilizing low oxidation states was observed to slow down the rate of photocatalytic hydrogen evolution.47, 48 In that system, the potential of the Co(II)/Co(I) couple is however more positive than for cobaloxime so that process (iii), not (ii), is rate-determining. Consequently, the electron-withdrawing phosphine ligand decreases the rate of H_2 evolution catalysis and initial rates for light-driven H_2 evolution.

Factors governing the stability against degradation (process iv) of reduced cobaloxime derivatives, including hydridocobaloximes are still unclear. We recently showed using time-resolved X-ray absorption spectroscopy that, in some cases, Co(I) species that accumulate under photocatalytic conditions22 are not catalytically active. The mechanism for such degradation is still under investigation, although it may be attributed to hydride transfer from the metal center to the ligand, competing catalytic H_2 evolution.49, 50 In that perspect, the fastest catalysts are less prone to degradation. The more nucleophilic hydride species indeed preferably reacts with protons, rather than migrating to the ligand, causing deactivation. This results in increased total turnover number, as observed with the stronger axial ligands in this study.39 Such a rational however does not stand for the diimine-dioxime cobalt system,47, 48 in which stabilization of the low valent redox states by electron-withdrawing phosphine ligand is accompanied by an increase of the total turnover number. While more studies are needed to fully understand the reactivity of intermediate species in this popular, though complex, series of catalysts, it seems clear that electron-rich ligands positioned in *trans* position to the hydride enhance its electron density and therefore its nucleophilicity/hydridicity, favoring protonation and H_2 evolution over hydride transfer and resulting in higher stability of the catalytic system.

Conclusions

In this study we have for the first time investigated different cobaloximes with various axial ligands as catalysts in photocatalytic hydrogen production. This systematic study shows a subtle influence of axial ligands on the performances of the system, both in terms of initial catalytic rate and overall catalytic stability. Weak axial ligands display rapid initial catalysis but result in low stability. By contrast, stronger axial ligands induce a reduced initial rate, but a better long-term stability. Further studies are still needed to fully understand the nature of the degradative process. In that prospect, the use of various techniques such as time-resolved X-ray absorption spectroscopies20–22 may be very valuable to identify all species at work during catalysis.

Experimental Section

Materials

All chemicals were purchased from the usual commercial sources and used as received.

Spectroscopy

^{1}H NMR spectra were recorded on Bruker AMX-500 MHz and Bruker DPX-300 MHz spectrometers as solutions in deuterated solvents by using the solvent peak as the internal standard. UV-Vis absorption spectra were measured on a Shimadzu UV-1700

spectrophotometer using 10 mm path-length cuvettes. IR spectra were recorded on Bruker IFS 66 spectrometer.

Electrochemistry

Cyclic voltammetry experiments were carried out at room temperature using an SP-300 Bio-Logic potentiostat. All measurements were carried out in DMF with a solute concentration of ca. 1.0 mM in the presence of tetrabutylammonium tetrafluoroborate (0.1 M) as supporting electrolyte. A three-electrode cell setup was used with a glassy carbon working electrode, a silver/silver chloride reference electrode, and a platinum wire as counter electrode. All potentials are reported versus the ferrocene/ferricinium couple added in the electrolyte at the end of each measurement.

Synthesis of the Photosensitizer

The dye $[ZnTMPyP]^{4+}Cl^{-}_{4}$ (**PS**) were synthesized according to the literature.51

General synthesis of catalysts 1-10

The general synthesis of cobalt complexes with dimethylglyoxime, $[Co(dmgH)_2(L)(L')]$ is described in the literature.33 $CoCl_2{\cdot}6H_2O$ (500 mg, 2.15 mmol), dimethylglyoxime (551 mg, 4.70 mmol), and NaOH (86.0 mg, 2.15 mmol) were dissolved in 95% ethanol (20 mL) and heated to 70°C. Ligand (L) (2.15 mmol) was then added and the resulting solution cooled to room temperature. A stream of air was then passed through the solution for 30 min, which caused precipitation of a brown solid. The suspension was stirred for 1 h and filtered. The precipitate was successively washed with water (5 mL), ethanol (2 x 5 mL), and diethyl ether (3 x 5 mL). The product was then extracted with acetone. Removal of the solvent from the extracts yielded pure complex.

Synthesis of the $[Co(dmgH)_2(4\text{-}CN\text{-}py)Cl]$ (1)

4-cyano-pyridine used as the axial ligand yielding the desired complex with 87%. Anal. Calcd for $C_{14}H_{18}ClCoN_6O_4$: C, 39.22; H, 4.23; N, 19.60. Found: C, 39.14; H, 4.28; N, 19.53. ^{1}H NMR (500 MHz, $CDCl_3$): δ= 18.12 (broad, OH), 8.53 (d, J = 6.7 Hz, 2H), 7.47 (d, J = 6.7 Hz, 2H), 2.41 (s, 12H). ^{13}C NMR (125 MHz, $CDCl_3$): δ=153.27, 152.51, 127.32, 123.73, 114.57, 13.37.

Synthesis of $[Co(dmgH)_2(4\text{-}COOH\text{-}py)Cl]$ (2)

4-carboxy-pyridine used as the axial ligand yielding the desired complex with 58%. Anal. Calcd for $C_{14}H_{19}ClCoN_5O_6$: C, 37.56; H, 4.28; N, 15.64. Found: C, 37.44; H, 4.35; N, 15.72. ^{1}H NMR (300 MHz, DMSO): δ=18.44 (s, 2H, OH), 14.14 (s, 1H, OH), 8.21 (d, J = 6.1 Hz, 2H), 7.85 (d, J = 6.0 Hz, 2H), 2.31 (s, 12H). ^{13}C NMR (75 MHz, DMSO): δ= 164.61, 152.73, 151.37, 141.17, 125.17, 12.70.

Synthesis of $[Co(dmgH)_2(py)Cl]$ (3)

Pyridine used as the axial ligand yielding the desired complex with 52%. Anal. Calcd for $C_{13}H_{19}ClCoN_5O_4$: C, 38.68; H, 4.74; N, 17.35. Found: C, 38.74; H, 4.61; N, 17.30. ^{1}H NMR (300 MHz, $CDCl_3$): δ=18.20 (broad, OH), 8.27 (d, J = 5.4 Hz, 2H), 7.70 (t, J = 7.5

Hz, 1H), 7.22 (d, *J* = 7.0 Hz, 2H), 2.40 (s, 12H). ^{13}C NMR (75 MHz, $CDCl_3$): δ=152.73, 151.21, 139.03, 125.78, 13.24.

Synthesis of [Co(dmgH)$_2$(4-SH-py)Cl] (4)

4-thiolo-pyridine used as the axial ligand yielding the desired complex with 61%. Anal. Calcd for $C_{13}H_{19}ClCoN_5O_4S$: C, 35.83; H, 4.39; N, 16.07. Found: C, 35.93; H, 4.23; N, 16.12. ^{1}H NMR (300 MHz, DMSO): δ= 18.25 (broad, 4H), 14.45 (broad, 1H), 8.12 (d, *J* = 5.9 Hz, 2H), 7.52 (d, *J* = 7.1 Hz, 2H), 2.25 (s, 12H). ^{13}C NMR (75 MHz, DMSO): δ=173.88, 150.33, 149.25, 127.36, 12.38.

Synthesis of [Co(dmgH)$_2$(4-CH$_3$-py)Cl] (5)

4-methyl-pyridine used as the axial ligand yielding the desired complex with 89%. Anal. Calcd for $C_{14}H_{21}ClCoN_5O_4$: C, 40.25; H, 5.07; N, 16.77. Found: C, 40.32; H, 4.99; N, 16.65. ^{1}H NMR (300 MHz, $CDCl_3$): δ=18.30 (broad, OH), 8.07 (d, *J* = 6.1 Hz, 2H), 7.01 (d, *J* = 5.8 Hz, 2H), 2.36 (d, *J* = 15.1 Hz, 12H), 2.32 (s, 3H). ^{13}C NMR (75 MHz, $CDCl_3$): δ=152.56, 151.47, 150.34, 126.77, 21.00, 13.20.

Synthesis of [Co(dmgH)$_2$(4-NH$_2$-py)Cl] (6)

4-amino-pyridine used as the axial ligand yielding the desired complex with 28%. Anal. Calcd for $C_{13}H_{20}ClCoN_6O_4$: C, 37.29; H, 4.81; N, 20.07. Found: C, 37.20; H, 4.94; N, 19.99. ^{1}H NMR (300 MHz, DMSO): δ=19.33 (broad, OH), 7.61 (s, 2H), 6.74 (s, 2H), 6.33 (s, 2H, NH_2), 2.47 (s, 12H). ^{13}C NMR (75 MHz, DMSO): δ= 165.53, 152.73, 150.57, 115.11, 12.67.

Synthesis of [Co(dmgH)$_2$(4-OH-py)Cl] (7)

4-hydroxy-pyridine used as the axial ligand yielding the desired complex with 26%. Anal. Calcd for $C_{13}H_{19}ClCoN_5O_5$: C, 37.20; H, 4.56; N, 16.69. Found: C, 37.12; H, 4.65; N, 16.65. ^{1}H NMR (300 MHz, DMSO): δ=18.49 (s, 2H, OH), 11.80 (s, 1H, OH), 7.65 (s, 2H), 6.79 (s, 2H), 2.32 (s, 12H). ^{13}C NMR (75 MHz, DMSO): δ=166.60, 152.18, 150.68, 114.17, 12.55.

Synthesis of [Co(dmgH)$_2$(imidazole)Cl] (8)

Imidazole used as the axial ligand yielding the desired complex with 77%. Anal. Calcd for $C_{11}H_{18}ClCoN_6O_4$: C, 33.64; H, 4.62; N, 21.40. Found: C, 33.52; H, 4.73; N, 21.30. ^{1}H NMR (300 MHz, DMSO): δ=18.67 (s, 2H, OH), 12.78 (s, 1H), 7.28 (s, 1H), 7.08 (s, 1H), 6.43 (s, 1H), 2.30 (s, 12H). ^{13}C NMR (75 MHz, DMSO): δ=151.40, 136.21, 125.84, 118.98, 12.42.

Synthesis of [Co(dmgH)$_2$(N-methyl-imidazole)Cl] (9)

N-methyl-imidazole used as the axial ligand yielding the desired complex with 78%. Anal. Calcd for $C_{12}H_{20}ClCoN_6O_4$: C, 35.44; H, 4.96; N, 20.66. Found: C, 35.36; H, 4.98; N, 20.55. ^{1}H NMR (300 MHz, $CDCl_3$): δ=18.46 (broad, OH), 6.69 (d, *J* = 15.7 Hz, 2H), 3.60 (s, 3H), 2.38 (s, 12H). ^{13}C NMR (75 MHz, $CDCl_3$): δ=151.93, 137.89, 128.60, 122.05, 35.20, 13.06.

Synthesis of [Co(dmgH$_2$)(dmgH)Cl$_2$] (10)

$CoCl_2 \cdot 6H_2O$ (500 mg, 2.15 mmol) dissolved in acetone (17mL). Dimethylglyoxime (551 mg, 4.70 mmol) was then added and the resulting solution stirred at room temperature for 20 minutes and filtered. The product was then extracted with acetone. Removal of the solvent from the extracts yielded pure **10** with 72%. Anal. Calcd for $C_8H_{14}C_{l2}CoN_4O_4$: C, 26.69; H, 3.92; N, 15.56. Found: C, 26.79; H, 3.84; N, 15.42. ^{1}H NMR (300 MHz, DMSO): δ=7.98 (broad, OH), 2.34 (s, 12H). ^{13}C NMR (75 MHz, DMSO): δ=149.60, 12.31.

Hydrogen production measurements

For photoinduced hydrogen evolution, each sample was prepared in a 30 mL Schlenck flask. Prior to sample preparation, an aqueous solution of TEOA (10% vol) was adjusted to pH=7 using conc.HCl. The components were then dissolved in 10 mL of a 1:1 (v/v) mixture of acetonitrile= and the aqueous TEOA (10%) solution. The sample flask was sealed with a Suba-seal septum and degassed by bubbling nitrogen through the solution for 20 min at room temperature. The samples were irradiated with a 500 W Xenon lamp using a cutoff filter designed to remove all light with λ < 440 nm. The amounts of hydrogen evolved were determined by gas chromatography (external standard technique) using a Shimadzu GC-2010 plus chromatograph with a TCD detector and a molecular sieve 5 Å column (30m-0.53 mm). Control experiments were run under the same conditions as the hydrogen evolution experiments with the removal of one of the components of the hydrogen generating samples.

For some control experiments a filter assembly was used consisting of a narrow bandpass filter at 572nm (bandwidth about 10nm FWHM) and a color-glass filter KG5. The color-glass filter transmits almost everything between 330 and 700nm but blocks the deep UV and IR radiation of the lamp. Extra care was taken to prevent stray UV light from reaching the sample by covering the area around the filter assembly with a large black carton.

An excess of mercury (ca 30eq) was added to our in order to investigate the effect of mercury during hydrogen production. More particularly, hydrogen production was not affected by the presence of mercury in the reaction mixture indicating that metallic cobalt particles are not formed as active catalytic species during the experiment. Metallic mercury remains shiny without forming an amalgam.

For the hydrogen evolution experiments the conditions were as follows: Hydrogen production upon irradiation (λ>440nm) of solution (Acetonitrile-TEOAaq (10%, pH 7) (1:1 v/v) containing **1** (4.0×10^{-5}M) and the respective catalyst (4.9×10^{-4}M). In the case of the experiments containing TiO_2 the procedure was the following. A solution of 2 (0.1 μmol in 0.5mL of TEOA, 10% v/v, pH 7) was added to a stirred dispersion of TiO_2 (20mg in 1mL TEOA). The mixture was left stirring for 1 h, was then centrifuged, and the filtered, clear supernatant was then analysed by UV-vis spectrophotometry. The amount of 2 adsorbed to TiO_2 was quantified by the absorbance difference at 244 nm before and after exposure to TiO_2 nanoparticles. The amount adsorbed to TiO_2 particles after 1 h was 89 ± 2 %.26

Supplementary Material

Refer to Web version on PubMed Central for supplementary material.

Acknowledgments

This work was supported by the European Commission's Seventh Framework Programme (FP7/2007-2013) under grant agreement n.° 229927 (FP7-REGPOT-2008-1, Project BIOSOLENUTI) and ERC Grant Agreement n.306398 (Project photocat**H**$_2$ode), Heraklitos grant from Ministry of Education, Special Research Account of the University of Crete, GSRT and the French National Research Agency (Labex program, ARCANE, ANR-11-LABX-0003-01). The COST Action CM1202 PERSPECT-H2O is also acknowledged for support via a short term scientific mission to France for AP.

References

1. Lewis NS, Nocera DG. Proceedings of the National Academy of Sciences. 2006; 103:15729–15735.
2. Thapper A, Styring SA, Saracco G, Rutherford AW, Robert B, Magnuson A, Lubitz W, Llobet AA, Kurz P, Holzwarth AR, Fiechter S, et al. Green. 2013; 3:43–57.
3. Cook TR, Dogutan DK, Reece SY, Surendranath Y, Teets TS, Nocera DG. Chemical Reviews. 2010; 110:6474–6502. [PubMed: 21062098]
4. Wang M, Sun L. ChemSusChem. 2010; 3:551–554. [PubMed: 20446339]
5. Du P, Eisenberg R. Energy & Environmental Science. 2012; 5:6012–6021.
6. Ladomenou K, Natali M, Iengo E, Charalampidis G, Scandola F, Coutsolelos AG. Coordination Chemistry Reviews.
7. Darwent JR, Douglas P, Harriman A, Porter G, Richoux M-C. Coordination Chemistry Reviews. 1982; 44:83–126.
8. Artero V, Chavarot-Kerlidou M, Fontecave M. Angewandte Chemie International Edition. 2011; 50:7238–7266. [PubMed: 21748828]
9. Wang X, Goeb S, Ji Z, Pogulaichenko NA, Castellano FN. Inorganic Chemistry. 2011; 50:705–707. [PubMed: 21204549]
10. Lazarides T, McCormick T, Du P, Luo G, Lindley B, Eisenberg R. Journal of the American Chemical Society. 2009; 131:9192–9194. [PubMed: 19566094]
11. Zhang P, Wang M, Li C, Li X, Dong J, Sun L. Chemical Communications. 2010; 46:8806–8808. [PubMed: 20957270]
12. Du P, Schneider J, Luo G, Brennessel WW, Eisenberg R. Inorganic Chemistry. 2009; 48:4952–4962. [PubMed: 19397296]
13. Guttentag M, Rodenberg A, Bachmann C, Senn A, Hamm P, Alberto R. Dalton Transactions. 2013; 42:334–337. [PubMed: 23090353]
14. Peuntinger K, Lazarides T, Dafnomili D, Charalambidis G, Landrou G, Kahnt A, Sabatini RP, McCamant DW, Gryko DT, Coutsolelos AG, Guldi DM. The Journal of Physical Chemistry C. 2012; 117:1647–1655.
15. Fihri A, Artero V, Razavet M, Baffert C, Leibl W, Fontecave M. Angewandte Chemie International Edition. 2008; 47:564–567. [PubMed: 18095368]
16. Fihri A, Artero V, Pereira A, Fontecave M. Dalton Transactions. 2008:5567–5569. [PubMed: 18854893]
17. Baffert C, Artero V, Fontecave M. Inorganic Chemistry. 2007; 46:1817–1824. [PubMed: 17269760]
18. Razavet M, Artero V, Fontecave M. Inorganic Chemistry. 2005; 44:4786–4795. [PubMed: 15962987]
19. Valdez CN, Dempsey JL, Brunschwig BS, Winkler JR, Gray HB. Proceedings of the National Academy of Sciences. 2012; 109:15589–15593.

20. Smolentsev G, Guda A, Zhang X, Haldrup K, Andreiadis ES, Chavarot-Kerlidou M, Canton SE, Nachtegaal M, Artero V, Sundstrom V. The Journal of Physical Chemistry C. 2013; 117:17367–17375.
21. Smolentsev G, Guda AA, Janousch M, Frieh C, Jud G, Zamponi F, Chavarot-Kerlidou M, Artero V, van Bokhoven JA, Nachtegaal M. Faraday Discuss. 2014; 171:259–273. [PubMed: 25415460]
22. Smolentsev G, Cecconi B, Guda A, Chavarot-Kerlidou M, van Bokhoven JA, Nachtegaal M, Artero V. Chemistry – A European Journal. 2015 n/a-n/a.
23. Dempsey JL, Brunschwig BS, Winkler JR, Gray HB. Acc Chem Res. 2009; 42:1995–2004. [PubMed: 19928840]
24. Marinescu SC, Winkler JR, Gray HB. Proceedings of the National Academy of Sciences. 2012; 109:15127–15131.
25. Dempsey JL, Winkler JR, Gray HB. Journal of the American Chemical Society. 2010; 132:1060–1065. [PubMed: 20043639]
26. Lakadamyali F, Reisner E. Chemical Communications. 2011; 47:1695–1697. [PubMed: 21212905]
27. Lv Y, Willkomm J, Leskes M, Steiner A, King TC, Gan L, Reisner E, Wood PT, Wright DS. Chemistry – A European Journal. 2012; 18:11867–11870.
28. Lakadamyali F, Reynal A, Kato M, Durrant JR, Reisner E. Chemistry – A European Journal. 2012; 18:15464–15475.
29. Natali M, Argazzi R, Chiorboli C, Iengo E, Scandola F. Chemistry – A European Journal. 2013; 19:9261–9271.
30. Natali M, Orlandi M, Chiorboli C, Iengo E, Bertolasi V, Scandola F. Photochemical & Photobiological Sciences. 2013; 12:1749–1753. [PubMed: 23900713]
31. Lazarides T, Delor M, Sazanovich IV, McCormick TM, Georgakaki I, Charalambidis G, Weinstein JA, Coutsolelos AG. Chemical Communications. 2013; 50:521–523. [PubMed: 23938601]
32. McCormick TM, Calitree BD, Orchard A, Kraut ND, Bright FV, Detty MR, Eisenberg R. J Am Chem Soc. 2010; 132:15480–15483. [PubMed: 20945839]
33. Schrauzer, GN., Parshall, GW., Wonchoba, ER. Inorganic Syntheses. Editon edn. John Wiley & Sons, Inc; 2007. p. 61-70.
34. Ramesh P, SubbiahPandi A, Jothi P, Revathi C, Dayalan A. Acta Crystallographica Section E. 2008; 64:m300–m301.
35. Rutherford PE, Thornton DA. Spectrochimica Acta Part A: Molecular Spectroscopy. 1979; 35:711–714.
36. Reynal A, Willkomm J, Muresan NM, Lakadamyali F, Planells M, Reisner E, Durrant JR. Chem Commun. 2014; 50:12768–12771.
37. Kaljurand I, Kütt A, Sooväli L, Rodima T, Mäemets V, Leito I, Koppel IA. The Journal of Organic Chemistry. 2005; 70:1019–1028. [PubMed: 15675863]
38. Chen MWC, Yeh A, Tsai TYR. Inorg Chim Acta. 1998:81–86.
39. Wakerley DW, Reisner E. Physical Chemistry Chemical Physics. 2014; 16:5739–5746. [PubMed: 24525821]
40. Kalyanasundaram K, Neumann-Spallart M. The Journal of Physical Chemistry. 1982; 86:5163–5169.
41. Muckerman JT, Fujita E. Chem Commun. 2011; 47:12456–12458.
42. Solis BH, Hammes-Schiffer S. Inorg Chem. 2011; 50:11252–11262. [PubMed: 21942543]
43. Artero V, Chavarot-Kerlidou M, Fontecave M. Angew Chem Int Ed Engl. 2011; 50:7238–7266. [PubMed: 21748828]
44. Benniston AC. Physical Chemistry Chemical Physics. 2007; 9:5739–5747. [PubMed: 19462568]
45. Solis BH, Yu Y, Hammes-Schiffer S. Inorg Chem. 2013; 52:6994–6999. [PubMed: 23701462]
46. Solis BH, Hammes-Schiffer S. Journal of the American Chemical Society. 2011; 133:19036–19039. [PubMed: 22032414]
47. Kaeffer N, Chavarot-Kerlidou M, Artero V. Accounts of Chemical Research. 2015; 48:1286–1295. [PubMed: 25941953]

48. Zhang P, Jacques P-A, Chavarot-Kerlidou M, Wang M, Sun L, Fontecave M, Artero V. Inorg Chem. 2012; 51:2115–2120. [PubMed: 22313315]
49. Simándi LI, Budó-Záhonyi É, Szeverényi Z. Inorganic and Nuclear Chemistry Letters. 1976; 12:237–241.
50. Simándi LI, Szeverényi Z, Budó-Záhonyi É. Inorganic and Nuclear Chemistry Letters. 1975; 11:773–777.
51. Christensen PA, Harriman A, Porter G, Neta P. Journal of the Chemical Society, Faraday Transactions 2: Molecular and Chemical Physics. 1984; 80:1451–1464.
52. Brown HC, Mihm XR. Journal of the American Chemical Society. 1955; 77:1723–1726.

Europe PMC Funders Author Manuscripts

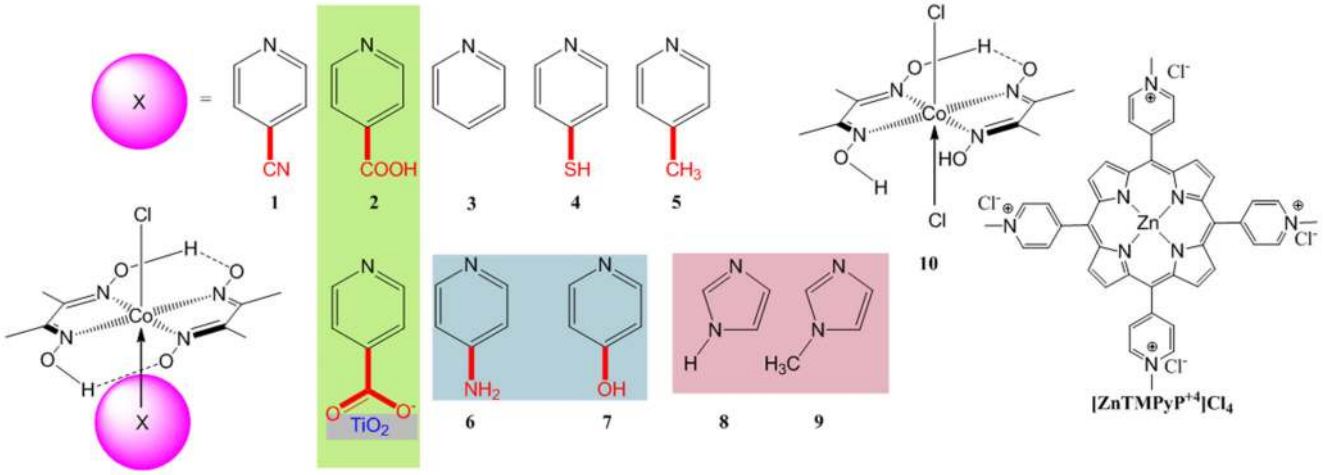

Figure 1.

Structures of *meso*-tetrakis (1-methylpyridinium-4-yl) porphyrin chloride ($[ZnTMPyP^{4+}]Cl_4$) and of the series of cobaloxime with different axial ligands **1-10** used in this study.

Europe PMC Funders Author Manuscripts

Europe PMC Funders Author Manuscripts

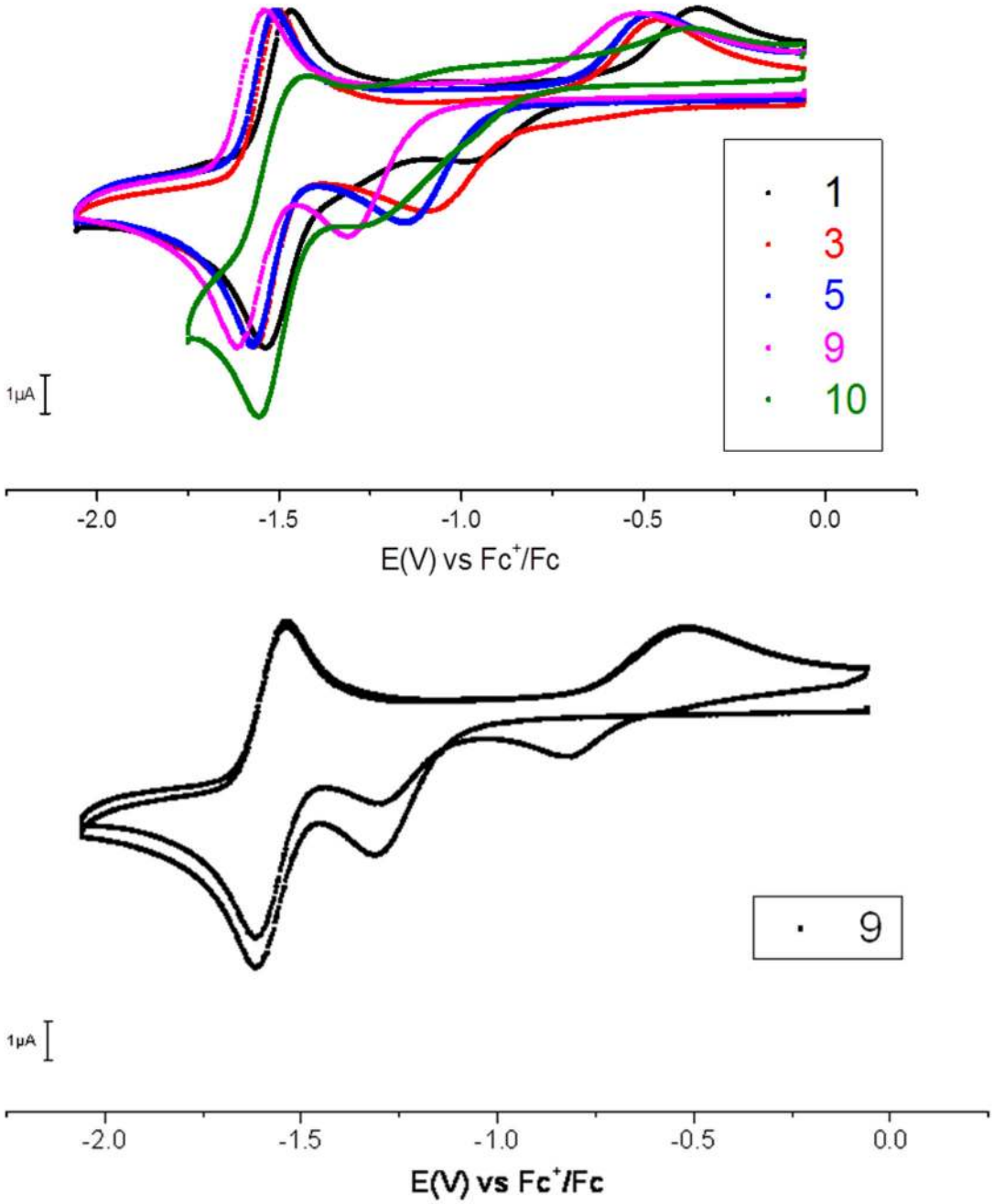

Figure 2.

top: Cyclic voltammograms of selected cobaloxime complexes (1mM, normalized with regards to the Co(II)/Co(I) signal of **3**) recorded in DMF (+ 0.1 mol.L^{-1} n-Bu_4NBF_4) at glassy carbon electrode (scan rate 100 mV.s^{-1})**;** bottom: first two cycles recorded under similar conditions as above with cobaloxime complex **9**.

Europe PMC Funders Author Manuscripts

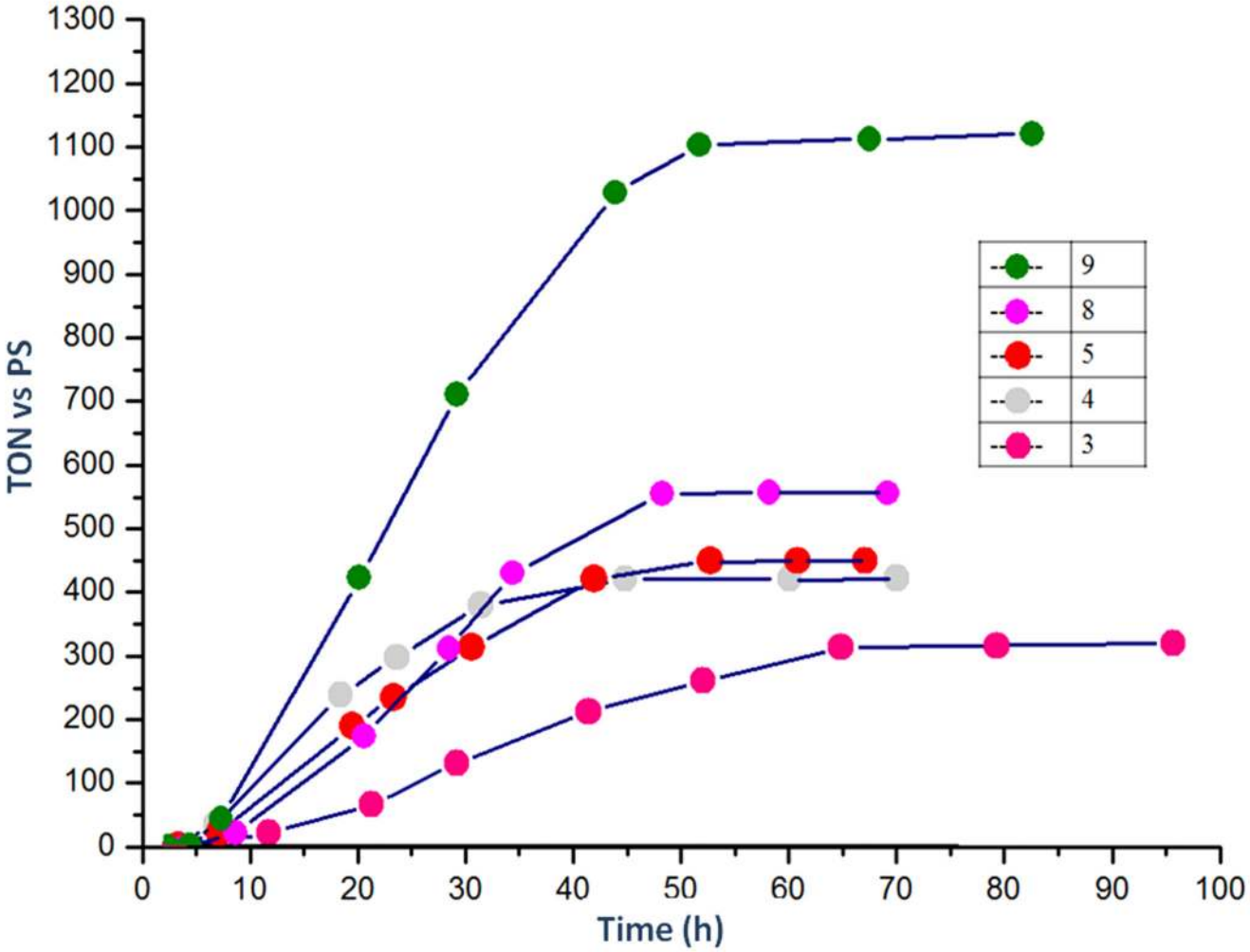

Figure 3.

Comparison of photocatalytic H_2 production of **3** with catalysts **4**, **5**, **8** and **9**. Conditions used are listed in Table 2 and experimental section.

Europe PMC Funders Author Manuscripts

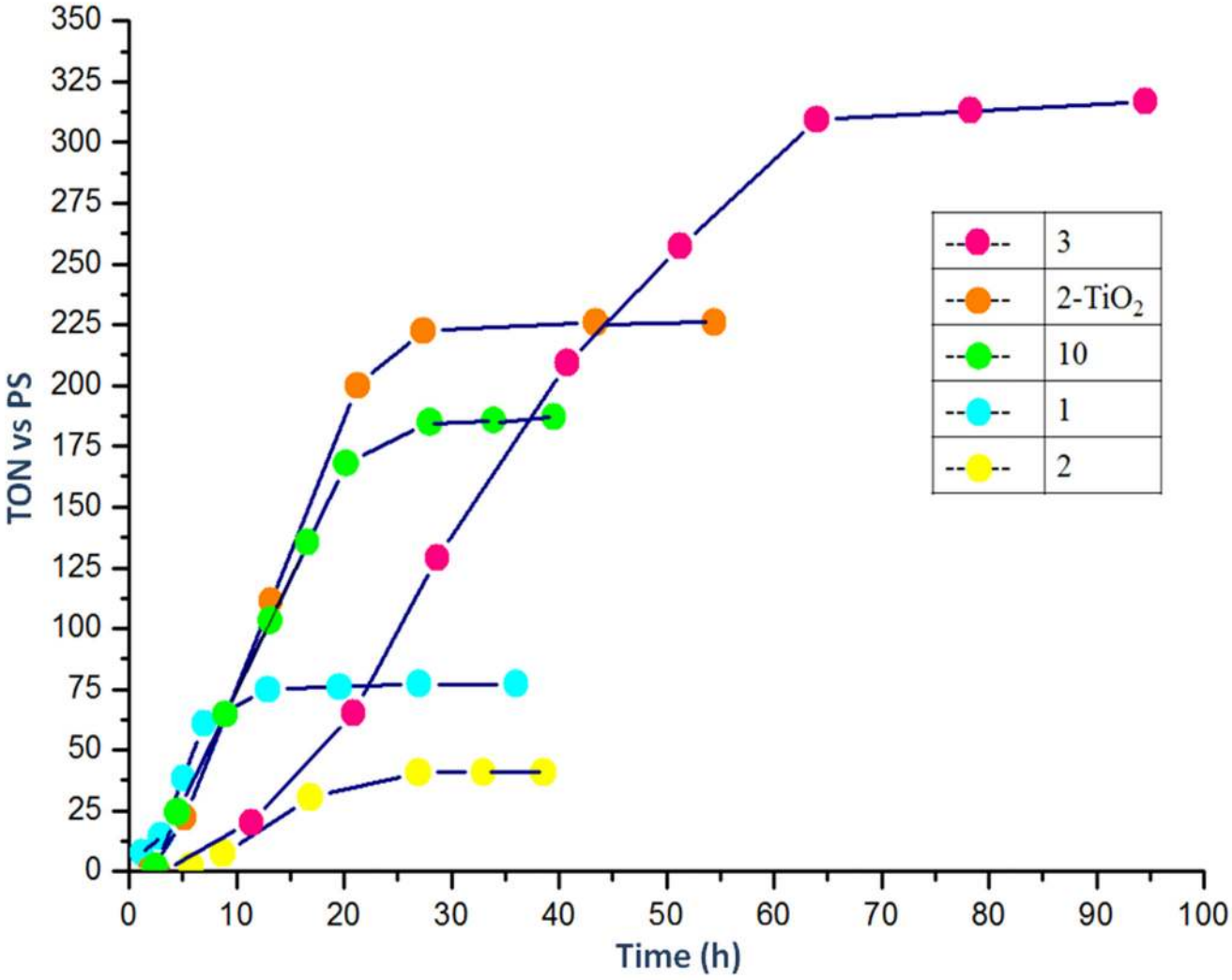

Figure 4.

Comparison of photocatalytic H_2 production of **3** with catalysts **1**, **2**, and **10**. Conditions used are listed in Table 2 and experimental section.

Europe PMC Funders Author Manuscripts

Table 1

IR spectral data for catalysts, pK_a52 of corresponding axial ligands in water, and redox potentials of their Co(III)/Co(II) (irrev) and Co(II)/Co(I) (rev.) processes.

Catalyst	pK_a	ν̄ Co-N_{axial} (cm^{-1})	ν Co-Cl (cm^{-1})	E (V vs Fc^+/Fc)	
				E_{pc} Co(III)/Co(II)	(E_{pc}+E_{pa})/2 Co(II)/Co(I)
1	1.90	435	428	–0.98	–1.50
2	4.18	441	428	–1.11	–1.55
3	5.22	455	420	–1.10	–1.53
4[2]	5.30	480	419	–1.09[1]	–1.59
5	6.02	483	418	–1.15	–1.54
6[3]	9.17	515	416	–1.08	–1.61
7[2]	11.0	507	409	–1.17	–1.55 (–1.65)[4]
8	6.90	495	413	–1.26	–1.58
9	7.40	503	412	–1.31	–1.57
10	-		414	–1.29	–1.52

[1] additional processes in this region assigned to thiol/ disulfide transition

[2] low solubilty

[3] low electrochemical response despite good solubility

[4] two reversible processes indicating the presence of isomeric species.

Europe PMC Funders Author Manuscripts

Table 2

Photocatalytic Hydrogen Production Using Different Cobaloximes as the Catalysts

Catalyst	pKa	TON	TOF (h^{-1})	Time for reaching plateau (h)
1	1.90	77	10	11
2	4.18	40	2	26
2-TiO_2	-	223	9	29
3	5.22	320	8	63
4	5.30	425	12	43
5	6.02	443	9	40
6	9.17	-	-	-
7	11.0	-	-	-
8	6.90	565	11	50
9	7.40	1135	23	50
10	-	290	10	23

[1]Difference for the TON with the previously work31 is due to the use of a slightly different setup for the photocatalytic process (a new reactor with 12 positions has been built). Therefore, the irradiation conditions are not exactly the same.

Conditions: Hydrogen production upon irradiation (λ>440nm) of solution (Acetonitrile-10% aqueous solution of TEOA (1:1 v/v) adjusted to pH=7 using $HCl_{conc.}$ containing PS (4.0×10^{-5}M) and the respective catalyst (4.9×10^{-4} M). The ratio PS / catalyst is 0.082.